

CT findings of small cell lung carcinoma

Can recognizable features be found?

Dongjun Lee, MD^a, Ji Young Rho, MD^{a,*}, Seunghun Kang, MD^a, Koun Joy Yoo, MD^b, Hye Jeong Choi, MD^c

Abstract

The purpose of this study was to clarify the recognizable computed tomography (CT) features of small cell lung carcinoma (SCLC).

Contrast enhanced CT scans were reviewed retrospectively for mass location, mediastinal extension, and other concomitant findings in 142 patients with pathologically proven SCLC. SCLC was classified into hilar mass only (type I), hilar mass with ipsilateral mediastinal extension (type II), hilar mass with bilateral mediastinal extension (type III), and peripheral mass (type IV). When mediastinal lymphadenopathy (m-LAP) was indistinguishable from a hilar mass, we defined it as a mediastinal conglomerate mass (m-CM). Type IIa or IIb had ipsilateral or bilateral m-LAP and type IIb, IIb or IIc had ipsilateral or bilateral m-CM.

Type I (n=8, 5.6%), type II (n=58, 40.8%), type III (n=55, 38.8%), and type IV (n=21, 14.8%) were manifested. The combination of a hilar mass and m-CM was found in 68 patients (47.9%). Type IV masses showed lobulation in 11, microlobulation in 4, both lobulated and irregular margins in 4, and spiculation in 2. A total of 120 patients (84.5%) had a bronchial stenosis/obstruction; single (n=52) and 2 or more (n=68). Ninety-five patients (67.0%) had vascular invasion including main/lobar pulmonary artery and superior vena cava, and 55 (38.7%) had pleural effusion and/or pleural nodules. Concomitant parenchymal findings (n=92, 64.8%) were noted: contiguous consolidation/nodule (n=45), hematogeneous spread (n=32), lymphangitic spread (n=21), obstructive pneumonia (n=22), and obstructive atelectasis (n=14).

In conclusion, the recognizable CT features of SCLC were a hilar mass with m-CM. Most of the hilar masses showed 2 or more bronchial stenoses/obstructions. Most cases of peripheral SCLC manifested as a lobulated mass rather than a spiculated mass. Vascular invasion and concomitant parenchymal findings were observed commonly.

Abbreviations: CT = computed tomography, m-CM = mediastinal conglomerate mass, m-LAP = mediastinal lymphadenopathy, MRI = magnetic resonance imaging, NSCLC = nonsmall cell lung carcinoma, PA = pulmonary artery, PET = positron emission tomography, SCLC = small cell lung carcinoma, SVC = superior vena cava.

Keywords: CT, diagnosis, lung, neoplasm, small cell lung carcinoma

1. Introduction

Small cell lung carcinoma (SCLC) accounts for 15% to 20% of all lung cancers and is the most common pulmonary neuroendocrine neoplasm that includes typical carcinoid, which is a low-grade malignancy, atypical carcinoid, which is a medium-grade malignancy, and large cell neuroendocrine carcinoma and SCLC, which are high-grade malignancies.^[1–5] SCLC is more aggressive

than non-small cell lung carcinoma (NSCLC) and is characterized by a rapid doubling time, high growth fraction (the ratio of proliferating cells to total cells), and greater propensity for early development of widespread metastases.^[2] SCLC usually occurs in older men (60–70 years old) and is well known to be closely associated with smoking and has the worst prognosis among lung cancers, due to the rapidly growing characteristic with dissemination before the first diagnosis.^[1–3] Thus, early and accurate diagnosis is important for SCLC, particularly in limited and extensive stages, as different approaches are required for treatment.

Because 90% to 95% of SCLCs arise from lobar or main bronchi, the most common manifestation of SCLC is a large mass centrally located within the lung parenchyma or a mediastinal mass involving the hilum.^[2,3,5] However, SCLC may occasionally arise as a relatively small bronchial tumor.^[2] Contrast-enhanced computed tomography (CT) scans can be useful for the diagnosis and revealing the extent of mediastinal invasion. However, only a few studies have reported CT findings of SCLC.^[6–10] Pearlberg et al^[7] reported distribution of lymph node enlargement and frequency of other intrathoracic findings in 37 patients with SCLC, and Hashimoto et al^[9] reported the CT findings of parenchymal lesions such as central or peripheral tumor, obstructive pneumonia, major atelectasis, and tumor extension in 38 patients with SCLC. Furthermore, Kazawa et al^[10] classified 68 cases of SCLC into 8 types and reported several features of SCLC. However, the number of cases in those studies was small, and the classification was not well organized.

Editor: Sergio Gonzalez Bombardiere.

The authors have no funding and conflicts of interest to disclose.

^a Department of Radiology, CHA Bundang Medical Center, CHA University, Yatap-dong, Bundang-gu, Seongnam-si, Gyeonggi-do, ^b Department of Radiology, St. Mary Dain Hospital, Mangpo-dong, Youngtong-gu, Suwon-si,

^c Department of Radiology, Seoul National University Hospital, Daehak-ro, Jongno-gu, Seoul, Republic of Korea.

* Correspondence: Ji Young Rho, Department of Radiology, CHA Bundang Medical Center, CHA University, Yatap-dong, Bundang-gu, Seongnam-si, Gyeonggi-do, Republic of Korea (e-mail: rhochest@cha.ac.kr).

Copyright © 2016 the Author(s). Published by Wolters Kluwer Health, Inc. All rights reserved.

This is an open access article distributed under the terms of the Creative Commons Attribution-Non Commercial-No Derivatives License 4.0 (CCBY-NC-ND), where it is permissible to download and share the work provided it is properly cited. The work cannot be changed in any way or used commercially without permission from the journal.

Medicine (2016) 95:47(e5426)

Received: 30 May 2016 / Received in final form: 7 September 2016 / Accepted: 21 October 2016

<http://dx.doi.org/10.1097/MD.0000000000005426>

We newly classified the SCLC types according to tumor location and mediastinal extension on CT scans and identified recognizable CT features for predicting SCLC.

2. Materials and methods

2.1. Population

This study was approved by the Institutional Review Board of the CHA Bundang Medical Center, CHA University and conducted according to the 1975 Declaration of Helsinki. We initially recruited 147 patients with pathologically proven SCLC, but 5 were excluded because they did not undergo contrast-enhanced chest CT. We performed a retrospective analysis of contrast-enhanced chest CT obtained in 142 patients (114 men and 28 women; age, 35–89 years; mean age, 67.7 years) from March 2005 to December 2014. The pathological diagnosis of SCLC was obtained by flexible fiberoptic bronchoscopic biopsy (n=108), CT-guided percutaneous transthoracic needle biopsy (n=29), both flexible fiberoptic bronchoscopic biopsy and transthoracic needle biopsy (n=4), and other biopsies such as cervical/axillary lymph nodes or pleura (n=22). The average time interval between obtaining biopsy and acquiring chest CT in those patients was 7.9 days. A smoking history was detected in 109 patients (76.8%).

A total of 115 contrast-enhanced chest CT scans were obtained in all patients by 16-multidetector row CT (Somatom Sensation 16; Siemens Medical Solutions, Forchheim, Germany) or 64-multidetector row CT scanners (LightSpeed VCT; GE Healthcare, Milwaukee, WI, or Optima CT 660; GE Healthcare, Milwaukee, WI) in our institution. The CT parameters were as follows in our institution: 120 kVp, 20 to 80 mAs, 3 to 5 mm section thickness. Twenty-seven cases had CT scans taken from other institutions: 4-multidetector CT scanner (Asteion or Aquilion; Toshiba, Tokyo, Japan), 16-multidetector row CT (Somatom Emotion 16; Siemens Medical Solutions, Forchheim, Germany), 64-multidetector row CT scanners (LightSpeed VCT; GE Healthcare, Milwaukee, WI). 2- [Fluoro-18] fluoro-2-deoxy-D-glucose positron emission tomography (PET)/CT and brain magnetic resonance imaging (MRI) were also performed routinely to detect distant metastases. If PET/CT or brain MRI was unavailable, bone scan and abdominal CT or brain CT scans were performed.

The CT images were reviewed retrospectively by 2 radiologists (JYR with 15 and DL with 2 years of chest CT experience) who were not blinded to the clinical data. We used consensus interpretation rather than independent review of the images. Therefore, final decisions regarding the findings were determined by consensus.

2.2. Assessment of CT findings

2.2.1. Tumor location and mediastinal extension. We defined hilar tumors as those where the center of mass was within or proximal to the lobar-segmental bronchial lumen and peripheral tumors as those where the center of mass was within the peripheral lung parenchyma or distal to a segmental bronchus. Lymph nodes were considered enlarged if their short-axis diameter in the axial plane was ≥ 10 mm. When mediastinal lymphadenopathy (m-LAP) was indistinguishable from the hilar mass, we defined it as mediastinal conglomerate mass (m-CM). According to these criteria, we classified SCLC into 4 types (Fig. 1): Type I, which was only a hilar mass; type II, which was hilar mass with ipsilateral mediastinal extension; type III, which

was a hilar mass with contralateral mediastinal extension; and type IV, which was a peripheral mass with or without m-LAP. Among them, when ipsilateral or bilateral m-LAP was recognized as an independently enlarged lymph node, it was defined as type IIa or IIIa. When ipsilateral or bilateral m-LAP was indistinguishable from a hilar mass, so-called m-CM, it was defined as type IIb (Fig. 2), IIIb (Fig. 3), or IIIc (Fig. 4).

2.2.2. Airway and vascular involvement. Single or multiple central bronchial wall thickening with stenosis and/or obstruction was evaluated for airway involvement. The central airway included the trachea, main stem bronchi, bronchus intermedius, and lobar-segmental bronchi of each lobe. Vascular invasion included the superior vena cava (SVC), the main pulmonary artery (PA), and lobar PA but excluded other vascular structures, such as the segmental PA, superior and inferior pulmonary vein or cardiac chamber.

2.2.3. Pleural and concomitant parenchymal findings. Pleural effusion, pleural nodules, and/or thickening were evaluated. Additionally, parenchymal findings, such as contiguous consolidation or nodules, obstructive pneumonia, obstructive atelectasis, and hematolymphangitic spread, were evaluated. Contiguous consolidation or nodules from the hilar mass was considered direct parenchymal involvement by the tumor. Obstructive pneumonia was demonstrated as surrounding lung consolidation, presence of fluid-filled bronchi, CT angiogram sign, and mild volume loss. It can be difficult to differentiate a central tumor from surrounding lung consolidation. Obstructive atelectasis was considered peripheral atelectasis related to a bronchial obstruction and was demonstrated as wedge-like volume loss and lack of an air-bronchogram. Noncontiguous nodules or masses in the contralateral lung were considered hematogeneous metastases. Irregular or nodular peribronchovascular interstitial thickening, interlobular septal thickening, and centrilobular nodules with or without ground-glass opacity were considered lymphangitic spread.

2.3. Distant metastases

Staging work-up to detect distant metastases was reviewed.

3. Results

3.1. Tumor location and mediastinal extension

A hilar mass with ipsilateral mediastinal extension (type II, 40.8%) and a hilar mass with bilateral mediastinal extension (type III, 38.8%) were common (Table 1); type I (n=8), type IIa (n=32), type IIb (n=26), type IIIa (n=13), type IIIb (n=20), type IIIc (n=22), and type IV (n=21). The combination of a hilar mass and m-CM, suggestive of type IIb + type IIIb + type IIIc was found in 68 (47.9%) patients.

Eleven of 21 patients with type IV did not exhibit m-LAP. Of these, 20 peripheral tumors appeared as homogenous or heterogeneous well enhanced solid masses, and the remaining tumor appeared as a solid mass with an internal air-bronchogram. Eleven had well-defined and lobulated margins. Microlobulation in 4, both lobulated and irregular margins in 4, and spiculation in 2 were detected. Tumor sizes were 1.4–6.7 cm (mean, 34.8 cm), ≤ 3 cm (n=7), >3 cm (n=14). The tumors were located in the peripheral (n=8) and subpleural zones (n=13) of the lung: right upper lobe (n=8), right middle lobe (n=1), right lower lobe (n=5), and left upper lobe (n=7).

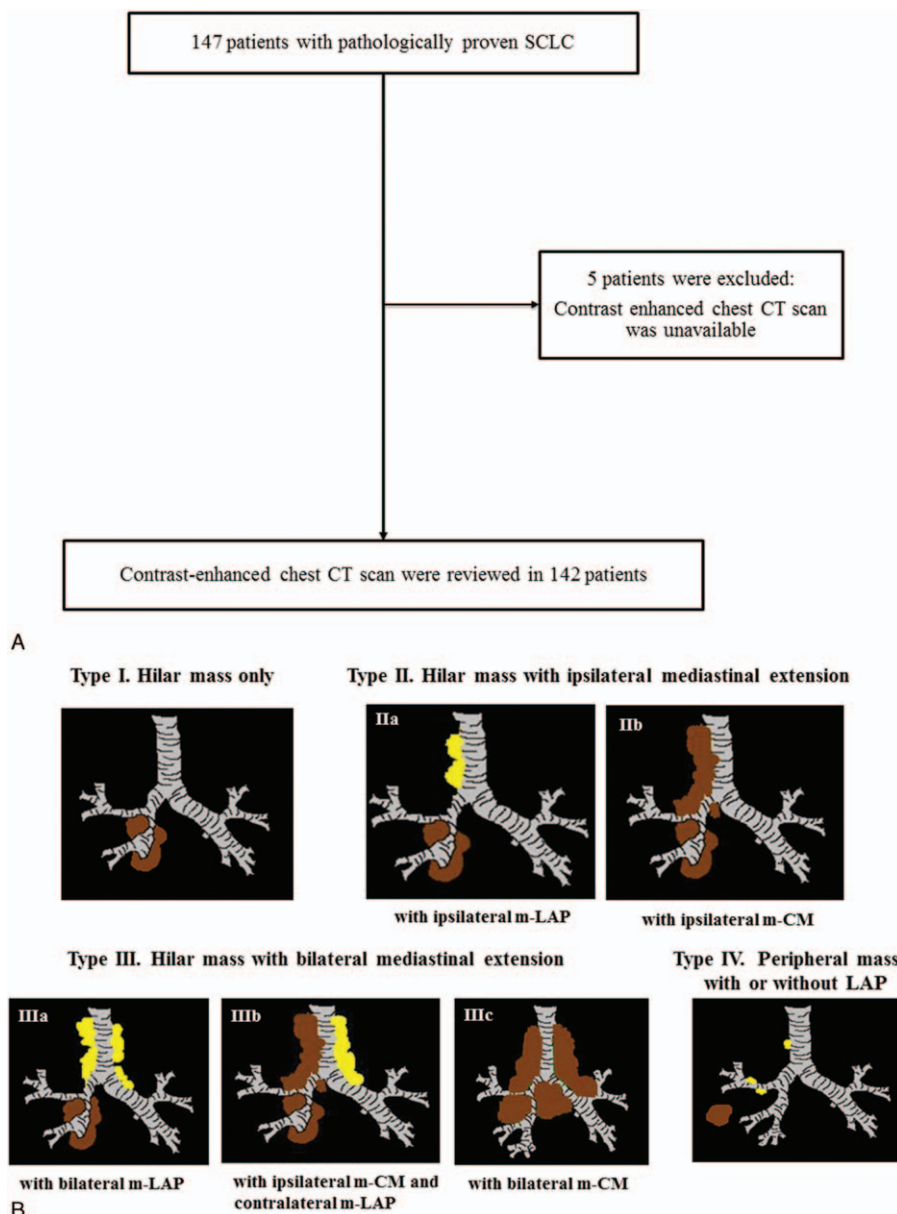


Figure 1. (A) Flow diagram of the patient selection process. (B) Schema for the 4 types of small cell lung carcinoma according to the tumor location and mediastinal extension. CT=computed tomography, m-CM=mediastinal conglomerate mass, m-LAP=mediastinal lymphadenopathy, SCLC=small cell lung carcinoma.

3.2. Airway and vascular involvement

A total of 120 patients (84.5%) had evidence of airway involvement (Table 2); 52 (43.4%) had single bronchial involvement and the remaining 68 (56.6%) had 2 or more bronchial involvement. Ninety-six of 277 affected bronchi involved a major airway such as trachea, both main stem bronchi, and the bronchus intermedius (Table 2). The combination of a hilar mass and m-CM (type IIb, IIIb, and IIIc) had an increased frequency of major airway involvement in 81 of 96 affected major airways (84.4%).

Ninety-five patients (67.0%) had evidence of vascular invasion (Table 2), such as only PA involvement (n=59), only SVC involvement (n=2), and a combination of PA and SVC involvement (n=34). PA involvement with or without SVC

invasion was the most manifested form of vascular involvement in 93 of 95 patients (97.8%). Only SVC involvement was rare (n=2, 2.1%).

3.3. Concomitant pleural and parenchymal findings

Pleural involvement was found in 55 patients (38.7%) (Table 3). Only pleural effusion was seen in 29 patients and contrast-enhanced pleural nodules with/without effusion were found in 26 patients.

Concomitant parenchymal lesions were found in 92 patients (64.8%); contiguous consolidation or nodules (n=45), haematogenous spread (n=32), lymphangitic spread (n=21), obstructive pneumonia (n=22), and obstructive atelectasis (n=14) (Table 3).

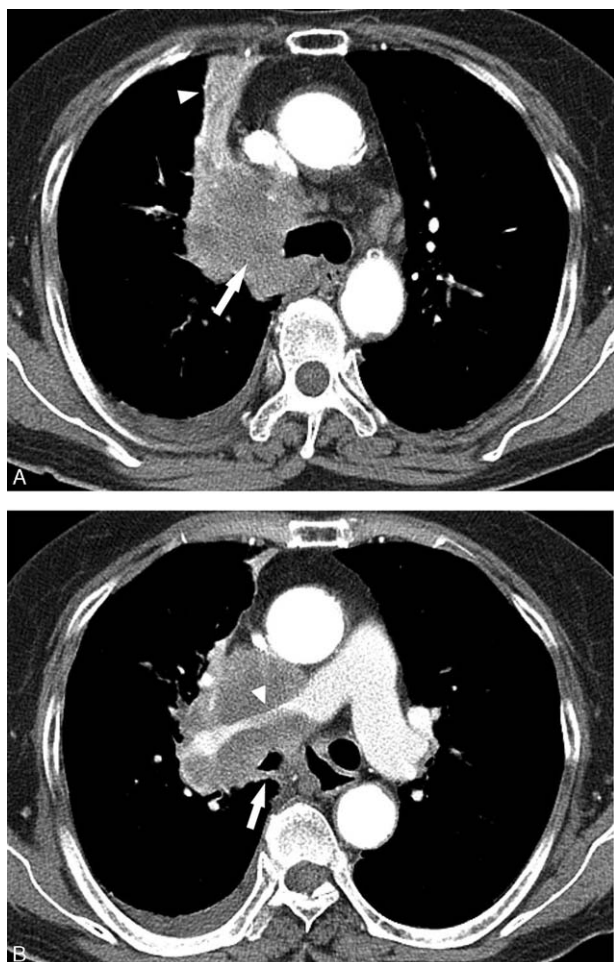


Figure 2. A 79-year-old female with SCLC (Type IIb). Axial CT mediastinal images show a right hilar with ipsilateral mediastinal conglomerate mass. (A) The mass occludes the right upper lobar bronchus (white arrow) and results in atelectasis of the right upper lobe (white arrowhead). (B) Note the encasement of the bronchus intermedius (white arrowhead) and right main pulmonary artery (white arrowhead) by the mass, resulting stenosis. CT=computed tomography, SCLC=small cell lung carcinoma.

3.4. Distant metastases

Extrathoracic distant metastases excluding the pleura and lung-to-lung metastases were found in 46 cases (32.4%); 1 in type I, 12 in type IIa, 7 in type IIb, 4 in type IIIa, 6 in type IIIb, 10 in type IIIc, and 6 in type IV. Distant metastases were recognized in the liver (n=24), bone (n=13), adrenal gland (n=11), brain (n=9), abdominal lymph nodes (n=6), neck lymph nodes (n=5), internal mammary lymph nodes (n=3), and axillary lymph nodes (n=1).

4. Discussion

Although understanding of CT manifestations of NSCLC has advanced, CT findings of SCLC have not been sufficiently reported.^[6–10] Hashimoto et al^[9] reviewed 38 patients with SCLC and detected bulky central masses as major CT findings, and most patients with central tumors showed bronchial narrowing. Kazawa et al^[10] classified 68 cases of SCLC into 8 types and reported common and rare types. Central perihilar type, central and mediastinal extension type, peripheral type, and

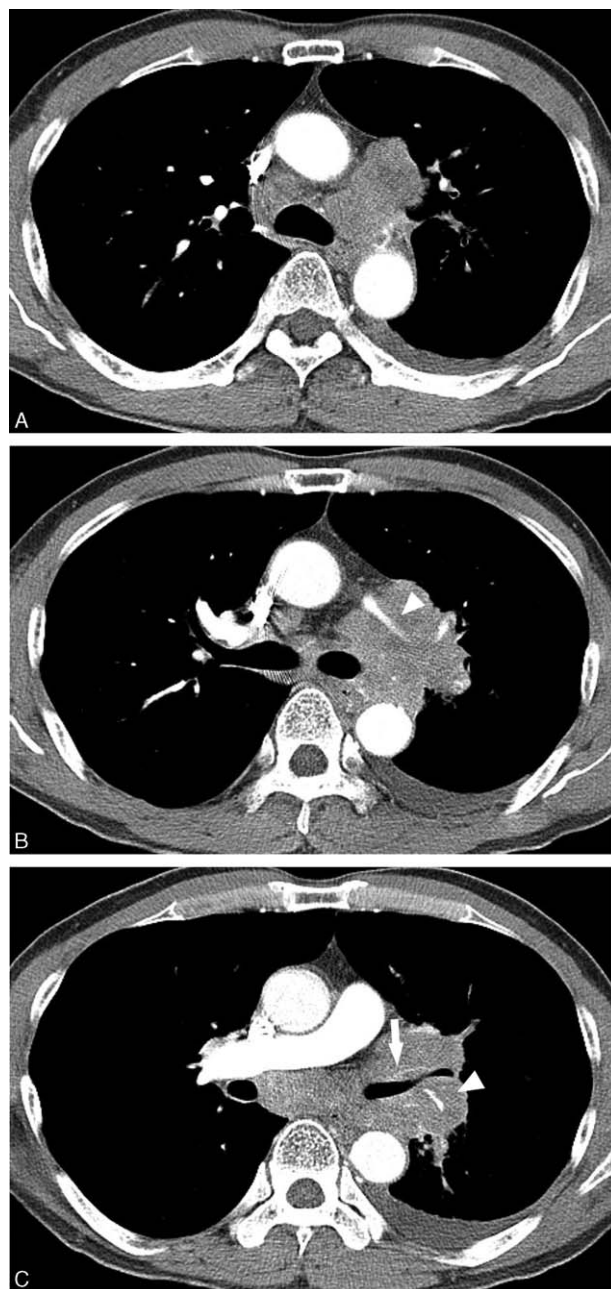


Figure 3. A 60-year-old male with SCLC (Type IIIb). (A, B, C) Axial CT mediastinal images show a left hilar mass with ipsilateral mediastinal conglomerate mass, encasing the left upper lobar bronchus (white arrow) and invading the left main and lobar pulmonary arteries (white arrowheads). Note the right lower paratracheal and subcarinal lymphadenopathies, and left pleural effusion. CT=computed tomography, SCLC=small cell lung carcinoma.

peripheral and mediastinal extension were frequently observed. However, the number of cases in those studies was small, and classification was not well organized. In the present study, SCLC was classified into 4 types according to tumor location and mediastinal extension on CT imaging. This classification is simple and easy to identify SCLC characteristics. m-LAP frequently forms a large mantle of soft tissue that infiltrates the mediastinum and encases the great vessels or extrinsically compresses the airway and cannot be reliably distinguished from a primary hilar



Figure 4. A 61-year-old female with SCLC (Type IIIc). (A, B, C) Axial CT mediastinal images show extensive bilateral mediastinal conglomerate mass, which could not be distinguished reliably from enlarged lymph nodes as a single mass, encasing and compressing the trachea to both main stem bronchi, and invading the superior vena cava (white arrowhead) and right main pulmonary artery (white arrow). CT=computed tomography, SCLC=small cell lung carcinoma.

tumor.^[9] We described this finding as m-CM, and subdivided mediastinal extension into distinguishable m-LAP and m-CM (Fig. 1). The most common type of SCLC found in this study was

type IIa, a central hilar mass with ipsilateral m-LAP (n=32, 22.5%) (Table 1). Type II cases were actually the most frequent (n=58, 40.8%), but there was similar frequencies of type II and type III (58 vs 55). In particular, the combination of a hilar mass with m-CM, suggestive of type IIb + type IIIb + type IIIc, was found in 68 (47.9%) patients. These results correspond to previous studies.^[8-10] Cotton studied bronchial extension in patients with bronchial carcinoma and found that submucosal tumor spread was noted in only 6% of lung carcinomas and had extensive mediastinal lymph node involvement.^[11] SCLC spreads predominantly in the submucosa and peribronchovascular connective tissue and invades the small blood vessels and lymphatics during the early stage.^[12] This pattern agrees with the results of our study. Therefore, we suggest that m-CM from a hilar tumor is a recognizable SCLC CT finding. In addition, type IV, which is a peripheral mass with or without LAP, was observed (n=21, 14.8%); 11 of the 21 patients did not exhibit m-LAP. Yabuuchi et al^[13] investigated 12 patients with surgically resected peripheral SCLC. All 12 tumors appeared as homogeneous masses, and 8 had well-defined margins. Lobulation was found in 7, marginal ground-glass opacity in 3, fine spiculation in 2, and ground-glass opacity and spiculation were detected in 1. Hashimoto et al^[14] reviewed the CT findings of 12 patients with peripheral SCLC, and most portions of the tumors in all patients consisted of a noncalcified solid mass. The tumor-marginal characteristics included a well-defined mass with a smooth surface (n=5), a well-defined mass with lobulation (n=3), and a mass with spiculation (n=4). Haque et al^[15] also reported that spiculation occurred in only 1 of 11 patients with peripheral SCLC and the remaining patients had smooth or lobulated borders. This finding is consistent with our study; well-defined and lobulated margin in 11, microlobulation in 4, both lobulated and irregular margins in 4, and spiculation in 2. We suggest that most peripheral SCLCs manifest as a well-defined lobulated mass rather than as a spiculated mass. However, these findings are nonspecific and similar to those of NSCLC.

We evaluated central airway involvement, including the trachea, main stem bronchi, bronchus intermedius, and lobar-segmental bronchi of each lobe. Grossly, SCLC trends to spread in the submucosa and peribronchovascular connective tissue, leading to obliteration of underlying airways and vessels.^[12] The endobronchial extension that is common in squamous cell carcinoma is seen less frequently, so the airway obstruction is usually caused by compression by the expanding tumor rather than by intraluminal obstruction.^[12] Previous studies^[6,7,9,10,15] reported that bronchial narrowing and wall thickening result from tumor spread into the submucosa of affected bronchi, mainly in the ipsilateral hilar bronchus. In the present study, airway involvement was very frequently observed (n=120, 84.5%) and 2 or more bronchi were more affected than a single bronchus (Table 2). Stenoses of the trachea to main stem bronchi or bronchus intermedius caused by a hilar mass with m-CM (type IIb, type IIIb, and type IIIc) were frequently (Table 2). Among concomitant parenchymal lesions, a bronchial obstruction with peripheral atelectasis was uncommon (Table 3). These results support submucosal tumor spread of SCLC and suggest that involvement of the major airway and 2 or more bronchi is a SCLC characteristic feature. Only 1 patient with type IIIb among all patients had no evidence of definite central airway invasion, except type IV. This patient showed nonspecific bronchoscopic findings, and SCLC was confirmed by lymph node biopsy.

Vascular invasion was observed in many cases (n=95, 67.0%) (Table 2). Kazawa et al^[10] reported that the tumor and m-LAP

Table 1

CT classification by tumor location and mediastinal extension in 142 patients with small cell lung carcinoma.

Classification of types of SCLC			
Type I Hilar mass only	8 (5.6%)		
Type II Hilar mass with ipsil. mediastinal extension	58 (40.8%)	a=with ipsil. m-LAP b=with ipsil. m-CM	32 (22.5%) 26 (18.3%)
Type III Hilar mass with bil. mediastinal extension	55 (38.8%)	a=with bil. m-LAP b=with ipsil. m-CM and contral. m-LAP c=with bil. m-CM	13 (9.2%) 20 (14.1%) 22 (15.5%)
Type IV Peripheral mass	21 (14.8%)		
Total, N	142		

bil = bilateral, contral=contralateral, CT = computed tomography, ipsil = ipsilateral, m-CM = mediastinal conglomerate mass, m-LAP = mediastinallymphadenopathy, SCLC = small cell lung carcinoma.

Table 2

CT findings of bronchial and vascular involvement in 142 patients with small cell lung carcinoma.

Type (n = 142)	Airway involvement (n = 120, 84.5%)							Vascular involvement (n = 95, 67.0%)		
	Single bronchus	Multiple bronchus	T	MB	BI	L/S	Total*	PA	PA+SVC	SVC
I, 8	6	2	0	1	0	9	10	4	0	0
II, 58	a	17	15	0	3	9	44	56	18	1
	b	12	14	5	9	8	35	57	15	9
III, 55	a	8	5	0	0	2	17	19	6	1
	b	6	13	1	7	6	30	44	13	5
	c	3	19	13	23	9	46	91	3	18
IV, 21	0	0	0	0	0	0	0	0	0	0
	52 (43.4%)	68 (56.6%)	19	43	34	181	277	59 (62.1%)	34 (35.8%)	2 (2.1%)

BI=bronchus intermedius, CT=computed tomography, L/S=lobar-segmental bronchus, MB=main stem bronchus, PA=pulmonary artery, SVC=superior vena cava, T=trachea. * number of affected airways.

are involved in the walls of vessel, such as the SVC or PA, in 44.1% of cases (SVC=32.3%, main PA=26.4%, main pulmonary vein = 16.1%, thoracic aorta = 10.3%). In the present study, we detected a higher frequency of vascular invasion, except to the pulmonary vein and aorta (Table 2). Main or lobar PA invasion with or without involvement of the SVC was a manifestation of vascular invasion (n=93, 97.8%), whereas invasion of only the SVC was rarely observed (n=2, 2.1%), which was probably due to the proximal location of the PA from the central airway where SCLC arises.

Accompanying pleural and parenchymal findings are helpful to identify and classify SCLC.

Kazawa et al^[10] grouped common and relatively rare types of SCLC. The characteristics of the rare type included lymphangitic spread, pleural dissemination, lobar replacement, and air-space

consolidation. However, we included these types as concomitant findings, so our classification of SCLC was easier. Pleural effusion was exclusively found in mediastinal extension cases of SCLC (type II or III). Only 1 case showed pleural effusion with nodules in type IV, and none in type I. Concomitant parenchymal findings were found in 92 patients (64.8%) (Table 3). Contiguous consolidation or nodules (n=45, 31.6%) was the most common parenchymal lesion. Obstructive pneumonia (n=22, 15.5%) or atelectasis (n=14, 9.9%) were infrequently found, and obstructive atelectasis was commonly associated with type II patients. These findings describe submucosal or peribronchial spread of SCLC.^[12] Hematogeneous spread (n=32, 22.5%), and lymphangitic spread (n=21, 14.8%) were also observed. Kazawa et al^[10] described lymphangitic spread as an unusual type, which was similar to our result.

Table 3

CT findings of pleural and concomitant parenchymal findings in 142 patients with small cell lung carcinoma.

Type (n = 142)	Pleural involvement (n = 55, 38.7%)		Concomitant parenchymal findings (n = 92, 64.8%)				
	Effusion	Nodule with/without effusion	Contiguous C/N	Hematogeneous spread	Lymphangitic spread	Obstructive pneumonia	Obstructive atelectasis
I, 8	0	0	1	0	0	2	0
II, 58	a	6	7	12	7	4	2
	b	6	4	10	3	6	3
III, 52	a	3	3	7	4	4	0
	b	7	6	6	7	2	8
	c	7	5	9	7	5	7
IV, 21	0	1	0	4	0	0	0
	29 (20.4%)	26 (18.3%)	45 (31.6%)	32 (22.5%)	21 (14.8%)	22 (15.5%)	14 (9.9%)

C/N=consolidation/nodule, CT=computed tomography.

Several limitations of this study should be mentioned. First, not all radiologically suspected nodular shadows, LAP, or distant metastatic lesions were pathologically confirmed. Second, we only evaluated patients with SCLC and did not consider differentiation of SCLC or NSCLC. Extensive NSCLC can also show a hilar mass with m-CM, so the CT features could overlap with those of SCLC. Although there are some overlapping features between these tumors, our results may be helpful for predicting SCLC. Third, several cases were difficult to classify, such as distinguishing m-LAP from m-CM was unclear in several cases.

In conclusion, we classified 4 general types of SCLCs and 7 types in detail on chest CT according to the mediastinal extension pattern, such as m-LAP and m-CM. A recognizable CT feature of SCLC was a central hilar tumor with bulky m-CM. Most cases with a hilar mass had 2 or more thickened bronchial wall with stenosis and/or obstruction. Vascular invasion and concomitant parenchymal lesions were commonly detected. In addition, most peripheral SCLCs manifested as a well-defined lobulated mass rather than a spiculated mass. These CT features of SCLC will improve early diagnosis for predicting SCLC and managing patients.

References

- [1] Sone S, Nakayama T, Honda T, et al. CT findings of early-stage small cell lung cancer in a low-dose CT screening programme. *Lung Cancer* 2007;56:207–15.
- [2] Carter BW, Glisson BS, Truong MT, et al. Small cell lung carcinoma: staging, imaging, and treatment considerations. *Radiographics* 2014;34:1707–21.
- [3] Benson RE, Rosado-de-Christenson ML, Martínez-Jiménez S, et al. Spectrum of pulmonary neuroendocrine proliferations and neoplasms. *Radiographics* 2013;33:1631–49.
- [4] Rekhman N. Neuroendocrine tumors of the lung: an update. *Arch Pathol Lab Med* 2010;134:1628–38.
- [5] Chong S, Lee KS, Chung MJ, et al. Neuroendocrine tumors of the lung: clinical, pathologic, and imaging findings. *Radiographics* 2006;26:41–57.
- [6] Whitley NO, Fuks JZ, McCrea ES, et al. Computed tomography of the chest in small cell lung cancer: potential new prognostic signs. *Am J Roentgenol* 1984;142:885–92.
- [7] Pearlberg JL, Sandler MA, Lewis JW Jr, et al. Small-cell bronchogenic carcinoma: CT evaluation. *Am J Roentgenol* 1988;150:265–8.
- [8] Ahn CS, Kim SJ, Choe KO. CT findings of small cell bronchogenic carcinoma. *J Korean Radiol Soc* 1991;27:358–62.
- [9] Hashimoto M, Heianna J, Okane K, et al. Small cell carcinoma of the lung: CT findings of parenchymal lesions. *Radiat Med* 1999;17:417–21.
- [10] Kazawa N, Kitaichi M, Hiraoka M, et al. Small cell lung carcinoma: Eight types of extension and spread on computed tomography. *J Comput Assist Tomogr* 2006;30:653–61.
- [11] Cotton RE. The bronchial spread of lung cancer. *Br J Dis Chest* 1959;53:142–50.
- [12] Fraser RG, Pare JAP, Pare PD, et al. *Diagnosis of Diseases of the Chest*. 3rd ed. Philadelphia:WB Saunders; 1989.
- [13] Yabuuchi H, Murayama S, Sakai S, et al. Resected peripheral small cell carcinoma of the lung: computed tomographic-histologic correlation. *J Thorac Imaging* 1999;14:105–8.
- [14] Hashimoto M, Miyauchi T, Heianna J, et al. Accurate diagnosis of peripheral small cell lung cancer with computed tomography. *Tohoku J Exp Med* 2009;217:217–21.
- [15] Haque N, Raza A, McGoey R, et al. Small cell lung cancer: time to diagnosis and treatment. *South Med J* 2012;105:418–23.